

all reactions studied, those with the residual nuclei in their ground states, lowest excited states, and even at higher excitations in the region of breakup reactions. This is inconsistent with current theoretical predictions based on pion stripping models,^{6,7} although most calculations for pion production to date do not include considerations of A_π .

The characteristics of the A_π suggest that its form is largely dictated by the reaction mechanism rather than by nuclear structure. The sign and simple angular structure of the observed analyzing power for these reactions is similar to the corresponding data for the reaction $p + p \rightarrow d + \pi^+$.¹⁵ Thus, the analyzing power in the nuclear pion production reaction appears to reflect the basic N - N pion-production analyzing power in the sense expected from an impulse approximation¹⁶ rather than being dominated by gross nuclear effects as expected from the single-nucleon models.

¹S. Dahlgren, B. Höistad, and P. Grafström, Phys. Lett. **35B**, 219 (1971).

²G. A. Miller, Nucl. Phys. **A224**, 269 (1974).

³L. D. Miller and H. J. Weber, Phys. Lett. **64B**, 279 (1976).

⁴B. Höistad, in Proceedings of the Topical Meeting on Intermediate Energy Physics, Zuos, Switzerland, 1976 (unpublished).

⁵H. W. Fearing, Phys. Rev. C **11**, 1210 (1975).

⁶W. R. Gibbs and S. Young, Phys. Rev. **17**, 837 (1978).

⁷J. V. Noble, Nucl. Phys. **A244**, 526 (1975).

⁸T. Bauer *et al.*, Phys. Lett. **69B**, 433 (1977).

⁹E. Heer, A. Roberts, and J. Tinlot, Phys. Rev. **111**, 640 (1958).

¹⁰G. Roy, J. Beveridge, and P. Bosman, in *Proceedings of the Fourth International Symposium on Polarization Phenomena in Nuclear Reactions, Zürich, 1975* (Birkhäuser-Verlag, Basel 1976), p. 862.

¹¹A complete description of the experimental arrangement will be published separately.

¹²S. Dahlgren, P. Grafström, B. Höistad, and A. Åsberg, Nucl. Phys. **A211**, 243 (1973).

¹³Madison Convention, in *Proceedings of the Third International Symposium on Polarization Phenomena in Nuclear Reactions, Madison, Wisconsin, 1970*, edited by H. H. Barschall and W. Haerberli (Univer. of Wisconsin Press, Madison, 1971).

¹⁴B. Höistad, in *Proceedings of the Seventh International Conference on High Energy Physics and Nuclear Structure, Zürich, Switzerland, 1977*, edited by M. P. Locker (Birkhäuser-Verlag, Basel, 1978).

¹⁵G. Jones, *Nucleon-Nucleon Interactions—1977*, AIP Conference Proceedings No. 41, edited by D. Measday, H. W. Fearing, and A. Strathdee, (American Institute of Physics, New York, 1978), p. 292.

¹⁶A. K. Kerman, H. McManus, and R. M. Thaler, Ann. Phys. (N.Y.) **8**, 551 (1959).

Effect of Nuclear Deformation on Heavy-Ion Fusion

R. G. Stokstad

The Weizmann Institute of Science, Rehovot, Israel, and Oak Ridge National Laboratory, Oak Ridge, Tennessee 37830

and

Y. Eisen, S. Kaplanis, D. Pelte, U. Smilansky, and I. Tserruya

The Weizmann Institute of Science, Rehovot, Israel

(Received 26 June 1978)

The cross sections for the fusion of ^{16}O with the spherical and deformed isotopes of Sm measured at bombarding energies spanning the fusion barrier indicate the importance of nuclear deformation for the fusion process. Calculations based on the usual static treatment of deformation effects, however, show significant discrepancies with the experimental data.

The deformation of one or both of the partners in a heavy-ion reaction is expected to influence the probability that the partners will fuse to form a compound nucleus. The effect on the fusion cross section is also expected to differ according to whether the deformation is static or dynamically induced.^{1,2} For a given bombarding

energy, the cross section for fusion with a rigid, deformed nucleus should exceed that of a comparable spherical nucleus when averaged over all initial orientations.^{1,3} Dynamic effects such as the excitation of vibrational states or the rotation of the deformed nucleus during the collision, however, are expected to reduce the fusion cross

section.^{1,2}

The above considerations have been the subject of theoretical study for some years. While much of this work has been motivated by an interest in the production of superheavy nuclei,⁴ the question of how nuclear deformation affects the fusion process is of general importance both for the study of nuclear reaction mechanisms and for the production of nuclei far from stability. Previous attempts to positively identify static deformation effects through the analysis of experimental data have either been inconclusive^{5,6} or have led to quite different conclusions.⁷ Dynamic effects are predicted to be relatively small^{1,2} and therefore have not been easily recognized.² The difficulty, as pointed out by Vaz and Alexander,⁶ has been a general lack of precision fusion data at subbarrier energies. In order to study the effects of deformation and to provide precise fusion cross sections, σ_{fus} , for testing the associated reaction theories we have measured σ_{fus} for $^{16}\text{O} + ^{148,150,152,154}\text{Sm}$. These isotopes of Sm span the transition region from spherical to strongly deformed ($\beta_2 \sim 0.3$) equilibrium shapes and, since their monopole Coulomb potentials are identical, they facilitate the isolation of effects depending on the shape of the nuclear surface. The use of heavy-ion projectiles as opposed to α particles greatly increases the sensitivity of the cross section to small changes in the fusion barrier while the doubly magic nature and consequent sphericity of ^{16}O simplifies the analysis. Most importantly, we have chosen an experimental technique which allows extension of the measurements to low bombarding energies and small cross sections.

The experiments were carried out using beams of ^{16}O ions provided by the 14 UD Pelletron accelerator at the Weizmann Institute. Thin targets (100–200 $\mu\text{g}/\text{cm}^2$) of isotopically enriched Sm (>95%) were prepared by vacuum evaporation onto thin carbon backings. The Yb evaporation residues were collected by a carbon foil of thickness 700–1000 $\mu\text{g}/\text{cm}^2$ located 2 mm behind the Sm target. Compound nuclei produced by the reaction of ^{16}O with the oxygen impurity in the target and with carbon passed through the catcher foil, resulting in a low background. Surface-barrier detectors placed at $\pm 40^\circ$ monitored the Rutherford scattering from the Sm target. Following bombardments of typically 30–60 minutes, the catcher foil was removed from the scattering chamber and placed before a 1.5-cm³ intrinsic Ge x-ray spectrometer. Spectra covering the range from 15 to 250 keV were then recorded

for successive counting intervals. The resolution at 50 keV was 360 eV FWHM (full width at half-maximum) which allowed separation of the $K\alpha_1, K\alpha_2$ lines of the x rays of Tm, Er, Ho, and Dy.

The radioactive isotopes of Yb and their daughters decay primarily by electron capture and the internal-conversion process in many cases further increases the already high yield of $K\alpha$ x rays. The absolute intensities of x rays from the radioactive sources were calculated from decay schemes in the Nuclear Data Sheets.⁸ The lifetimes of the adjacent isotopes are also sufficiently different that their individual contributions could be determined from the measured time dependence of the x-ray yield for parent and daughter activities.

The determination of the absolute cross section is based on the Rutherford cross section and the relative counting rates for elastically scattered ^{16}O ions in the monitor detectors and the post-bombardment x rays. Corrections have been applied for the summing of coincident radiations, electronic deadtime, fluctuations in beam current, and for energy loss in the target. The decay of the compound nucleus by charged-particle emission was found to be usually less than 5% and has been included in σ_{fus} ; the fission mode of decay is negligible at these low bombarding energies.⁹ In several cases, cross sections were deduced from γ -ray yields and confirmed the x-ray results. The standard deviation (random plus systematic errors) on the absolute cross sections is estimated at typically $\pm 10\%$. This error does not include a contribution from the $\pm 0.3\%$ uncertainty on the absolute ^{16}O beam energy. A detailed description of the experiment and deduction of absolute cross sections will be published separately.

Figure 1(a) presents the measured values of σ_{fus} . At the highest bombarding energy, the cross sections obtained for the different isotopes are almost identical. As the bombarding energy is reduced, however, σ_{fus} exhibits a systematic variation, with the more deformed isotopes exhibiting progressively larger cross sections relative to the less deformed isotopes. This systematic variation in the energy dependence of σ_{fus} for the different isotopes is in qualitative agreement with a static treatment of the effect of deformation.³ The observed effects, however, appear quite large—at 60 MeV, σ_{fus} for $^{16}\text{O} + ^{154}\text{Sm}$ exceeds that for $^{16}\text{O} + ^{148}\text{Sm}$ by a factor of 20. Since experimental errors are relatively small, a quantitative analysis as described in the follow-

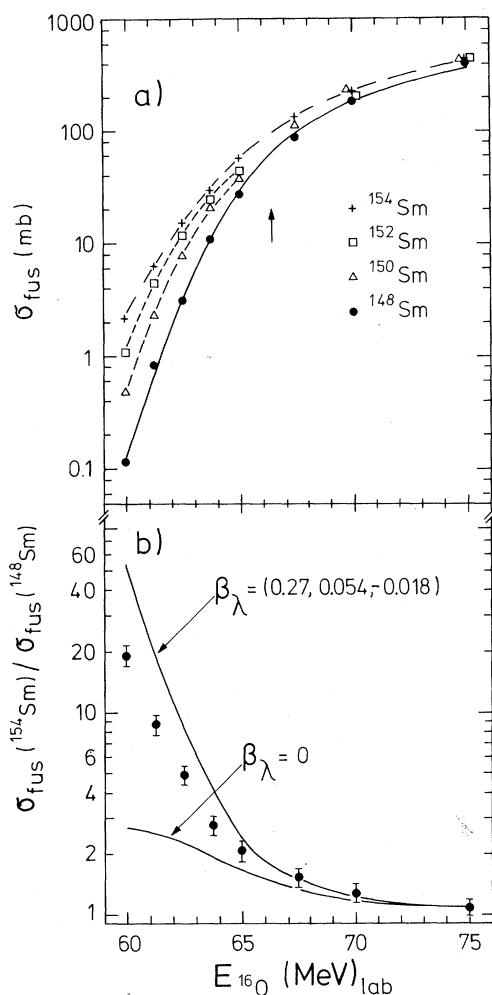


FIG. 1. (a) Values of σ_{fus} for $^{16}O + ^{148,150,152,154}Sm$ from $E_{lab} = 60-75$ MeV. The full curve connecting the ^{148}Sm data points is the result of a calculation described in the text. The other curves are to guide the eye. The arrow denotes the location in the lab system of the fusion barrier corresponding to V at $dV/dr = 0$ for $^{16}O + ^{148}Sm$. (b) The ratio of σ_{fus} for ^{154}Sm and ^{148}Sm . The full curves are the results of static calculations described in the text.

ing is possible.

The procedure thus far followed in the usual static fusion calculation^{3,5} is to replace the nuclear radius R in the expression for the nuclear potential V_n with a function of the form $R \rightarrow R(\theta) = R_p + R_T [1 + \sum_\lambda \beta_\lambda Y_\lambda^0(\theta)]$ where θ is the angle between the axis of symmetry of the deformed target nucleus and the initial direction of the spherical projectile. The total real potential is then taken to be

$$V_n(R(\theta), r) + V_C(\theta, r) + \frac{\hbar^2}{2\mu r^2} l(l+1), \quad (1)$$

where the angular dependence of the Coulomb potential $V_C(\theta, r)$ is determined by the multipole moments for a charge distribution with deformation parameters β_λ . The transmission coefficients for fusion, $T_l(\theta)$, in the expression,

$$\sigma_{fus}(\theta) = \pi \lambda^2 \sum_{l=1}^{\infty} (2l+1) T_l(\theta), \quad (2)$$

may be evaluated using methods varying in sophistication from the Hill-Wheeler expression for a parabolic approximation of the barrier³ to the solution of the Schrödinger equation for a complex potential in which the radius of the imaginary part is also angle dependent. Since the target nucleus is not aligned, an average over the initial orientations, $\sigma_{fus} = \int_0^{\pi/2} \sigma_{fus}(\theta) \sin \theta d\theta$, is performed.

Our procedure is to determine empirically an appropriate fusion potential for a spherical target by fitting the measured values of σ_{fus} for $^{16}O + ^{148}Sm$ assuming $\beta_\lambda = 0$. Such a semiempirical procedure is essential since theoretical predictions of the nuclear potential for fusion reactions generally are not sufficiently accurate for the prediction of subbarrier cross sections.⁷ The full curve through the data points in Fig. 1(a) represents the fusion cross section calculated with the Schrödinger equation and a complex potential having a liquid-drop form factor¹⁰ for the real potential ($V_0 = -36$ MeV, $r_0 = 1.0$ fm, $d = 2.5$ fm) and a rectangular well ($W = 10$ MeV, $r_0 = 1.3$) for the imaginary part. The values of β_λ deduced from α -particle inelastic scattering¹¹ were then used to predict σ_{fus} for the other isotopes. We will present a detailed comparison of such predictions with all of our experimental data in a future publication and concentrate here on a comparison of σ_{fus} for ^{148}Sm and ^{154}Sm .

Figure 1(b) shows the ratio of the fusion cross sections for ^{154}Sm and ^{148}Sm . The curve labeled with $\beta_\lambda = 0$ is the ratio obtained under the assumption that ^{154}Sm is also spherical with a radius which is larger than that of ^{148}Sm by an amount given by an $A^{1/3}$ dependence of R_T on nucleon number. The difference between this curve and unity represents the change in relative fusion cross section expected because of the slightly higher center-of-mass bombarding energy for ^{154}Sm and because of the larger radius which ^{154}Sm would have even in the absence of any deformation. The difference between the curve for $\beta_\lambda = 0$ and the experimental data represents the effect which we may associate with the different nuclear structures of ^{148}Sm and ^{154}Sm . The main difference be-

tween these nuclei is their vibrational (spherical) and rotational (deformed) nature, respectively.

The result of a calculation employing the measured¹¹ deformation parameters for ^{154}Sm and the above complex potential is shown in Fig. 1(b). (The values of β_λ used in conjunction with the present nuclear potential were obtained by the re-normalization procedure, $\beta r_0 = \text{const.}$ ¹¹) Not only does a static treatment of the reaction mechanism predict quite different energy dependencies for ^{148}Sm and ^{154}Sm , we see in Fig. 1(b) that it leads to a marked overestimate of the observed effect. In order to reproduce the experimental data, a value of $\beta_2 = 0.20$ (with $\beta_4 = \beta_6 = 0$) must be used for ^{154}Sm . This value is not consistent with the measured values and their errors.¹¹ A reduction of the radius parameter r_0 for ^{154}Sm by 0.6%, which corresponds to maintenance of constant volume under deformation, can account for only a small portion of this discrepancy. A reanalysis of the experimental data using $\beta_2 = 0.13$ for ^{148}Sm (which represents a root-mean-square amplitude of time-dependent deviations from sphericity¹¹) also leads to results very similar to those shown in Fig. 1(b). Furthermore, the failure of the calculation to reproduce the experimental data is not a consequence of the particular numerical procedure chosen to evaluate the transmission coefficients, $T_l(\theta)$, in Eq. (2). An analysis using the Hill-Wheeler³ approximation for the barrier penetrability (and hence no explicit imaginary potential) produces theoretical curves very similar to those shown in Fig. 1(b) provided that the spherical potential deduced in this approximation reproduces σ_{fus} for ^{148}Sm .

Some possible explanations for the discrepancy are found in the approximations embodied in the usual static treatment of deformation effects.

(i) For noncentral collisions, the separation of the nuclear surfaces also depends on the azimuthal orientation of the deformed nucleus with respect to the scattering plane. Equation (1) neglects this completely.

(ii) Equation (1) introduces a variation in nuclear potential solely through a shift in the radius with orientation. The strength of the nuclear potential may also vary with position along the nuclear surface through changes in the local radius of curvature.¹² The diffusivity of the nuclear surface has been assumed to be independent of θ .

(iii) Geometrical effects associated with the finite size of the projectile have been neglected.

(iv) The discrepancy in Fig. 1(b) may result in part from the neglect of dynamic effects. We

have estimated (using a quasistatic approximation) the importance of rotation prior to fusion and the loss of relative kinetic energy through excitation of rotational and vibrational degrees of freedom. The combined estimated effect of these processes results in a lowering of the predicted cross section at 60 MeV lab for ^{154}Sm by a factor of about 1.7. Comparable dynamic effects for $^{16}\text{O} + ^{148}\text{Sm}$, however, would also be present. Of the above considerations, item (i) appears to us to represent the most serious shortcoming of the usual static treatment of deformation effects. It would also be of interest to apply a coupled-channels analysis to the data.

In summary, a sizable variation in the energy dependence of the measured cross sections has been observed for the fusion of ^{16}O with the spherical and deformed isotopes of Sm. A comparison with a calculation of σ_{fus} using previously measured deformation parameters suggests that much of this variation can be attributed to the effects of static deformation. Significant differences between theory and experiment remain, however, and point toward necessary improvements in the theoretical treatment of the effect of deformation on heavy-ion fusion. The resultant progress in understanding the role of deformation in heavy-ion fusion could have important consequences for fusion reactions in mass regions quite apart from the Sm isotopes,¹³ and could eventually lead to application of measurements such as those presented here to problems in nuclear structure.

We are pleased to acknowledge stimulating discussion with Shimon Levit and Aage Winther, and the participation of David Shur in the data analysis. This work received support from the U. S. Department of Energy under contract with Union Carbide Corporation.

¹H. Holm, W. Scheid, and W. Greiner, Phys. Lett. **29B**, 473 (1969).

²P. W. Riesenfeldt and T. D. Thomas, Phys. Rev. C **2**, 711 (1970).

³C. Y. Wong, Phys. Rev. Lett. **31**, 766 (1973); J. O. Rasmussen and K. Sugawara-Tanabe, Nucl. Phys. **A171**, 497 (1971).

⁴R. Behringer, Phys. Rev. Lett. **18**, 1006 (1967).

⁵W. Scobel, A. Mingery, M. Blann, and H. H. Gutbrod, Phys. Rev. C **11**, 1701 (1975).

⁶L. C. Vaz and J. M. Alexander, Phys. Rev. C **10**, 464 (1974).

⁷H. Freiesleben and J. R. Huizenga, Nucl. Phys. **A224**, 503 (1974); J. M. Alexander, L. C. Vaz, and

S. Y. Lin, Phys. Rev. Lett. **33**, 1487 (1974).

⁸*Nuclear Data Sheets*, compiled by K. Way *et al.* (Printing and Publishing Office, National Academy of Sciences—National Research Council, Washington, D. C.).

⁹T. Sikkeland, Phys. Rev. **135**, B669 (1964).

¹⁰R. Bass, Nucl. Phys. **A231**, 45 (1974).

¹¹D. L. Hendrie *et al.*, Phys. Lett. **26B**, 127 (1968);
N. K. Glendenning *et al.*, Phys. Lett. **26B**, 131 (1968);

W. Brückner *et al.*, Nucl. Phys. **A231**, 159 (1974);
A. H. Shaw and J. S. Greenberg, Phys. Rev. C **10**, 263 (1974).

¹²J. Randrup and J. Vaagen, to be published; R. Bass, private communication.

¹³R. G. Stokstad, Z. E. Switkowski, R. A. Dayras, and R. M. Wieland Phys. Rev. Lett. **37**, 888 (1976);
M. Arnould and W. M. Howard, Nucl. Phys. **A272**, 295 (1976).

Isotope Distributions in the Reaction of ^{238}U with ^{238}U

M. Schädel, J. V. Kratz, H. Ahrens, W. Brüchle, G. Franz,
H. Gäggeler, I. Warnecke, and G. Wirth
Gesellschaft für Schwerionenforschung, D-61 Darmstadt, Germany

and

G. Herrmann,^(a) N. Trautmann, and M. Weis
Institut für Kernchemie, Universität Mainz, D-65 Mainz, Germany
(Received 22 May 1978)

Radiochemically determined cross sections $\sigma(Z, A)$ were used to construct charge and mass distributions for the reaction of 1785-MeV ^{238}U ions with thick ^{238}U targets. Fission of the colliding nuclei is found to dominate. For the surviving uraniumlike fragments an enhancement of yields compared to the Kr + U and Xe + U reactions is observed. The formation of heavy actinides is shown to be associated with the low-energy tails of the broad excitation energy distributions in damped collisions.

The mechanism of strongly damped collisions between very heavy nuclei is of great current interest.¹ The ^{238}U beam available at the Unilac accelerator is presently being used to investigate the $^{238}\text{U} + ^{238}\text{U}$ reaction with several complementary techniques. First results of $\Delta E, E$ counter telescope measurements were published by Hildenbrand *et al.*² The aim of the present work was (i) to extend earlier radiochemical studies³⁻⁶ of mass and charge distributions in reactions of ^{238}U with ^{40}Ar , ^{56}Fe , ^{84}Kr , and ^{136}Xe ions to the U + U system, and (ii) to learn about the prospects of synthesizing superheavy elements in the latter reaction. Therefore, particular emphasis was put on the investigation of the survival probability of heavy actinide isotopes after their formation in damped collisions.

The experiments were performed with ^{238}U beams of 7.5 MeV/amu and up to 2.5×10^{11} particles/s incident on a thick, water-cooled uranium metal target (300 mg/cm²). All reaction products are stopped in the target. After bombardment the target was dissolved and the reaction products were chemically separated into 25 fractions which were assayed for x-ray, γ -ray,

α -particle, and spontaneous-fission activities over a period of several months. From these data integral cross sections $\sigma(Z, A)$ for individual isotopes with Z ranging from 26 to 100 and half-lives from 23 min to 7.4×10^3 yr were obtained. The cross sections represent mean values between the incident energy and the interaction barrier (6.1 MeV/amu) and were calculated⁷ using an effective number of 1.5×10^{19} target atoms per square centimeter. The $\sigma(Z, A)$ values were used to define a surface of independent formation cross sections in a Z - A plane [see Fig. 1(b)]; the process to generate the surface was discussed in Ref. 3. Corrections for products from reactions of ^{238}U ions with ^{16}O target impurities were made, if necessary, as described elsewhere.⁷

We interpret the charge distribution, Fig. 1(a), as being due to the superposition of four components: (i) products around uranium from quasi-elastic transfer (890 mb), (ii) nuclides with Z from ~ 73 to 100 arising from an originally symmetric distribution in the binary deep-inelastic transfer (290 mb), (iii) a nearly symmetric fission-product distribution originating from the sequential fission of highly excited binary inelas-